

## Supporting Information

### **Modulation of the excited states of Ruthenium(II)-perylene dyad to access near-IR luminescence, long-lived perylene triplet state and singlet oxygen photosensitization**

Isabele S. Campos<sup>†</sup>, Andrea Fermi<sup>§</sup>, Barbara Ventura<sup>⊥</sup>, Carlos A. F. Moraes<sup>†</sup>, Gabriel H. Ribeiro<sup>†</sup>, Tiago Venâncio<sup>†</sup>, Paola Ceroni<sup>§\*</sup>, and Rose M. Carlos <sup>†</sup> \*

<sup>†</sup> *Departamento de Química, Universidade Federal de São Carlos, CP 676, CEP 13565-905, São Carlos-SP, Brazil*

<sup>§</sup> *Dipartimento di Chimica Ciamician, Alma Mater Studiorum - Università di Bologna, Via Selmi 2, 40126 Bologna, Italy*

<sup>⊥</sup> *Institute for Organic Synthesis and Photoreactivity (ISOF), National Research Council of Italy (CNR), Via P. Gobetti 101, I-40129 Bologna, Italy*

*\* Corresponding Author*

*\*Email:*

rosem@ufscar.br

paola.ceroni@unibo.it

## Table of Contents

### Materials and Methods

1. General Informations.....	S4
2. Synthetic Protocols and Characterization Details .....	S4
2.1. PDI-Py ligand (N,N'-Di(1,10-phenanthroline)-1,7-dipyrroli-dinylperylene-3,4:9,10-tetracarboxylic acid diimide).....	S4
2.2. RuPDI-Py dyad .....	S5
3. Steady State Absorption and Emission Studies in DMSO .....	S5
4. Solvatochromism.....	S6
Scheme S1. Synthetic route to PDI-Py ligand. ....	S7
Figure S1. ESI(+)-MS spectrum of PDI-Py ligand in methanol. ....	S7
Table S1. <sup>1</sup> H and <sup>13</sup> C NMR chemical shifts (δ) of the PDI-Py ligand in DMSO-d <sub>6</sub> at 600 MHz. ....	S7
Figure S2. (A) <sup>1</sup> H NMR spectrum of PDI-Py ligand in DMSO-d <sub>6</sub> at 298K, with insertion (B) of the deshielding region of the spectrum. Insertion of the chemical structure of PDI Py ligand. ...	S8
Figure S3. Aromatic region in the <sup>1</sup> H- <sup>1</sup> H COSY NMR spectrum of the PDI-Py ligand (600 MHz, DMSO-d <sub>6</sub> ). ....	S9
Figure S4. Aromatic region in the <sup>1</sup> H- <sup>13</sup> C HSQC NMR spectrum of the PDI-Py ligand (600 MHz, DMSO-d <sub>6</sub> ). ....	S9
Figure S5. Aromatic region in the <sup>1</sup> H- <sup>13</sup> C HMBC NMR spectrum of the PDI-Py ligand (600 MHz, DMSO-d <sub>6</sub> ). ....	S10
Scheme S2. Synthetic route to RuPDI-Py dyad. ....	S10
Figure S6. ESI(+)-MS spectrum of RuPDI-Py dyad in acetonitrile (top) and spectrum expansion on [M] <sup>2+</sup> ion, m/z =673.1649 highlighting Ruthenium isotopic distribution (bottom). ....	S11
Table S2. <sup>1</sup> H and <sup>13</sup> C NMR chemical shifts of the RuPDI-Py dyad in DMSO-d <sub>6</sub> at 600 MHz. ....	S12
Figure S8. Aromatic region in the <sup>1</sup> H- <sup>1</sup> H COSY NMR spectrum of the RuPDI-Py dyad (600 MHz, DMSO-d <sub>6</sub> ). ....	S14
Figure S9. Aromatic region in the <sup>1</sup> H- <sup>13</sup> C HSQC NMR spectrum of the RuPDI-Py dyad (600 MHz, DMSO-d <sub>6</sub> ). ....	S14

Figure S10. Aromatic region in the $^1\text{H}$ - $^{13}\text{C}$ HMBC NMR spectrum of the RuPDI-Py dyad (600 MHz, DMSO- $d_6$ ).	S15
Figure S11 – Comparison of the absorption (dashed black-line), emission (solid black line), and excitation (colored line) spectra of the PDI-Py (A) and RuPDI-Py (B) in deaerated DMSO solution ( $c = 20 \mu\text{M}$ ), except from excitation spectra that were registered for solutions with $A < 0.1$ in the investigated spectral range.	S15
Figure S12. Time-resolved emission profiles for PDI-Py (A) and RuPDI-Py (B) with $\lambda_{\text{EX}} = 640 \text{ nm}$ and $\lambda_{\text{EM}} = 780 \text{ nm}$ in deaerated DMSO solution ( $c = 20 \mu\text{M}$ ).	S16
Figure S13. Comparison of emission spectra of RuPDI-Py (red) and PDI-Py (green) obtained from optically matched solutions ( $\text{abs} = 0.1$ at the excitation wavelength) in deaerated DMSO solution. A: $\lambda_{\text{exc}} = 420 \text{ nm}$ ; B: $\lambda_{\text{exc}} = 640 \text{ nm}$ .	S16
Figure S14. Absorption, emission spectra and emission lifetime decay profiles of PDI-Py (A) and RuPDI-Py (B) in different organic solvents at room temperature (aerated solutions), and in butyronitrile glass at 77 K. The emission lifetimes were measured at $\lambda_{\text{exc}} = 640 \text{ nm}$ and $\lambda_{\text{em}} = 780 \text{ nm}$ in aerated solutions.	S17
Figure S15. Femtosecond transient absorption spectroscopy with $\lambda_{\text{exc}} = 450 \text{ nm}$ (A) and nanosecond transient absorption spectroscopy with $\lambda_{\text{exc}} = 355 \text{ nm}$ (B) of the $[\text{Ru}(\text{phen})_3]^{2+}$ reference in DMSO: spectral evolution and kinetic analysis at selected wavelengths.	S18
Figure S16. Spectral distribution of the amplitudes of the calculated lifetimes from global fitanalysis of the nanosecond transient absorption matrix of the RuPDI-Py dyad excited at 355 nm in DMSO under oxygen-free conditions.	S18
Figure S17. Cyclic voltammogram of PDI-Py (A) and RuPDI-Py (B) in $\text{CH}_3\text{CN}$ solutions at 2 V/s. TBAPF6 was used as a supporting electrolyte; ferrocene was added to the same solutions as in internal reference (0.40 V vs. SCE).	S19
Table S3. Halfwave potentials vs. SCE for the analysed compounds in $\text{CH}_3\text{CN}$ .	S19
Figure S18. Spectroelectrochemical analyses for PDI-Py and RuPDI-Py in degassed $\text{CH}_3\text{CN}$ at several applied potentials.	S20
Figure S19. Bleaching of DMA (100 $\mu\text{M}$ ) in DMSO upon irradiation at 450 nm in the presence of the RuPDI-Py dyad (A), PDI-Py ligand (B), $[\text{Ru}(\text{phen})_3]^{2+}$ reference (C), and DMA control (D) (irradiation time = 30 minutes).	S21
Figure S20. Bleaching of DMA in DMSO upon irradiation at 720 nm in the presence of the RuPDI-Py dyad (A), PDI-Py ligand (B), and DMA control (C) (irradiation time = 30 minutes).	S22
References	S22

## 1. General Informations

One- ( $^1\text{H}$ ) and two-dimensional NMR experiments ( $^1\text{H}$ - $^1\text{H}$  COSY,  $^1\text{H}$ - $^{13}\text{C}$  HSQC and  $^1\text{H}$ - $^{13}\text{C}$  HMBC) were measured in a DMSO- $\text{d}_6$  solution using Bruker Advance 600 MHz spectrometer. Mass spectrometric measurements were carried out in the positive mode on an Agilent 6545 qTOF MS mass spectrometer (Agilent Technologies, Santa Clara, CA, EUA) equipped with an electrospray ionization interface. The full-scan MS data were produced across the mass range of 150–1500 Da and 400–800 Da. Samples were prepared by dissolving the PDI-Py ligand in methanol and the RuPDI-Py dyad in acetonitrile (LC-MS grade) and subsequently diluted to concentrations of 10 ppm and 5 ppm. Solutions were introduced into the ESI source via direct infusion through a 250  $\mu\text{L}$  glass syringe. The ESI source conditions were as follows: capillary voltage 3.8 kV, sample cone voltage 700 V, cone gas flow ( $\text{N}_2$ ) 12  $\text{L}\cdot\text{min}^{-1}$ , desolvation gas flow 10  $\text{L}\cdot\text{min}^{-1}$ , source temperatures 80  $^\circ\text{C}$  and desolvation temperature was set to 320  $^\circ\text{C}$ . Mass Hunter Workstation v.B.08.00 software was used for data acquisition and processing.

## 2. Synthetic Protocols and Characterization Details

### 2.1. PDI-Py ligand (N,N'-Di(1,10-phenanthroline)-1,7-dipyrrolidinylperylene-3,4:9,10-tetracarboxylic acid diimide)

The starting material 1,7-dipyrrolidinylperylene-3,4:9,10-tetracarboxylic acid bisanhydride (1) was prepared according to the literature method.<sup>1</sup> The synthesis of the PDI-Py ligand was adapted from the previously reported methods for the structurally bay-substituted PDI compounds<sup>2</sup>, and it is detailed below.

A mixture of 5-amino-1,10-phenanthroline (0.083 g, 0.424 mmol) and 1,7-dipyrrolidinylperylene-3,4:9,10-tetracarboxylic acid bisanhydride (0.1 g, 0.188 mmol) was dissolved in a mixture of 3.0 ml pyridine and 3.0 g imidazole, and then set to reflux at 120  $^\circ\text{C}$  for 24 h under a nitrogen atmosphere. After cooling to room temperature, slow addition of the reaction mixture into 25 ml of 15% aqueous HCl solution yielded a green precipitate that was collected by gravimetric filtration and washed with 300 mL of water. The crude product was purified by column chromatography on silica gel using DCM/MeOH (85/15, v/v) as the eluent. The product was obtained as a dark green solid (0.113 g, 68%). MALDI-TOF MS  $m/z$  for  $\text{C}_{56}\text{H}_{36}\text{N}_8\text{O}_2$ ; calcd: 884.2860; found 885.2954 [ $\text{M} + \text{H}$ ] $^+$  and 443.1521 [ $\text{M} + 2\text{H}$ ] $^{2+}$ .  $^1\text{H}$  NMR (600 MHz, DMSO- $\text{d}_6$ )  $\delta$  9.23 [dd (4.3, 1.6 Hz); 2H;  $\text{H}_2$ ], 9.18 (m; 2H;  $\text{H}_9$ ), 8.58 [(dt (8.1, 1.8 Hz); 2H;  $\text{H}_4$ ), 8.47 - 8.40 (m; 6H;  $\text{H}_c$   $\text{H}_7/\text{H}_a$ ), 8.22 (s; 2H;  $\text{H}_6$ ), 7.88 [dd (8.1, 4.4 Hz); 2H;  $\text{H}_3$ ], 7.76 - 7.72 (m; 4H;  $\text{H}_b$ ,  $\text{H}_8$ ), 3.84 - 3.70 (m; 4H;  $\text{H}_{\text{Py}}$ ), 2.80 - 2.73 (m; 4H;  $\text{H}_{\text{Py}}$ ), 1.82 - 2.22 (m; 8H;  $\text{H}_{\text{Py}}$ ) ppm.

## 2.2. RuPDI-Py dyad

The precursor complex *cis*-[Ru(phen)<sub>2</sub>Cl<sub>2</sub>] (3) was prepared by dissolving RuCl<sub>3</sub>·3H<sub>2</sub>O (0.2 g, 0.765 mmol), 1,10-phenanthroline (0.28 g, 1.6 mmol) and LiCl (0.23 g, 5.44 mmol) in 15 mL of DMF, and then set to reflux for 8 h under a nitrogen atmosphere. After cooling to room temperature, the crude product was precipitated by addition of cold acetone and yielded a purple precipitate that was collected by vacuum filtration and washed with cold water and ethyl ether, and dried under vacuum. The product was obtained as a dark purple solid (0.12 g, 30%).

The RuPDI-Py dyad was prepared by dissolving *cis*-[Ru(phen)<sub>2</sub>Cl<sub>2</sub>] (0.036 g, 0.067 mmol) and PDI-Py (0.089 g, 0.1 mmol) in 7 mL of DMF, and then set to reflux for 24 h under a nitrogen atmosphere. After cooling to room temperature, ammonium hexafluorophosphate NH<sub>4</sub>PF<sub>6</sub> (0.022 g, 0.134 mmol) was added to the reaction mixture yielded a green precipitate that was collected by gravimetric filtration and washed with cold water and ethyl ether. The crude product was purified by successive recrystallizations in acetone and ethyl ether. The product was obtained as a green solid (0.063 g, 67%). MALDI-TOF MS *m/z* for C<sub>73</sub>H<sub>52</sub>N<sub>12</sub>O<sub>4</sub>Ru; calcd: 1346.3278; found 673.1649 [M]<sup>2+</sup> and 449.1137 [M + H]<sup>3+</sup>. <sup>1</sup>H NMR (600 MHz, DMSO-*d*<sub>6</sub>) δ 9.23 (m; 1H; H<sub>2</sub>), 9.18 (m; 1H; H<sub>9</sub>), 8.88 – 8.74 (m; 6H; H<sub>2'</sub>, H<sub>9'</sub>, H<sub>2''/H<sub>9''</sub></sub>), 8.64 (m; 1H; H<sub>6'</sub>), 8.58 (m; 1H; H<sub>4</sub>), 8.50 – 8.35 (m; 9H; H<sub>7</sub>, H<sub>5''</sub>, H<sub>6''</sub>, H<sub>a</sub>, H<sub>a'</sub>, H<sub>c</sub>, H<sub>c'</sub>), 8.27 - 8.09 (m; 7H; H<sub>6</sub>, H<sub>4'/H<sub>7'</sub></sub>, H<sub>4''/H<sub>7''</sub></sub>), 7.94 – 7.65 (m; 10H; H<sub>3</sub>, H<sub>8</sub>, H<sub>3''</sub>, H<sub>8''</sub>, H<sub>3'</sub>, H<sub>8'</sub>, H<sub>b</sub>, H<sub>b'</sub>), 3.87 – 3.71 (m; 4H; H<sub>Py</sub>), 2.97 - 2.70 (m; 4H; H<sub>Py</sub>), 2.18 – 1.85 (m; 8H; H<sub>Py'</sub>) ppm.

## 3. Steady State Absorption and Emission Studies in DMSO

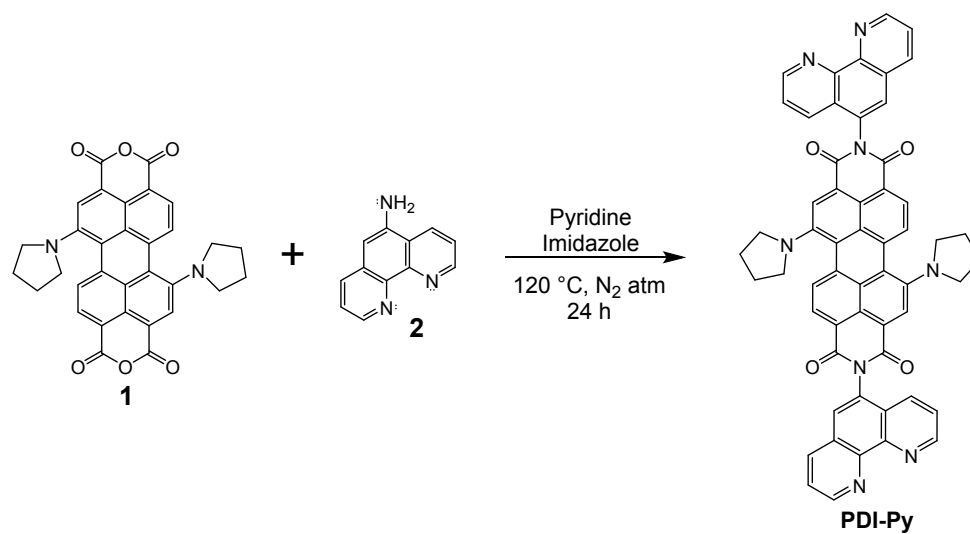
To investigate a possible energy transfer mechanism from the {[Ru(phen)<sub>3</sub>]<sup>2+</sup>} to the {PDI-Py} unit, the excitation spectrum of the dyad at λ<sub>EM</sub> = 780 nm was compared to the absorption spectrum (Figure S11b). The excitation spectrum resembles the absorption profile of PDI-Py rather than that of the dyad. Furthermore, a comparison of the emission spectra of optically matched solutions of the RuPDI-Py dyad and PDI-Py showed that when the {PDI-Py} component is selectively excited at 640 nm, the fluorescence intensity of <sup>1</sup>PDI-Py in the dyad is the same as that of PDI-Py (Figure S13). Meanwhile, using excitation at 420 nm, where the amount of light absorbed by the {PDI-Py} is 60%, the fluorescence yield of <sup>1</sup>PDI-Py in the dyad decreases by 25% compared with that of the PDI-Py reference. These results indicate that when the dyad is excited in the region where only the {PDI-Py} component absorbs light the usual PDI-Py fluorescence is observed, leading to exclude significant interactions between {PDI-Py} and {[Ru(phen)<sub>3</sub>]<sup>2+</sup>} moieties in the excited state. On the other hand, when the dyad is excited where both moieties absorb light, the PDI-Py fluorescence is promoted only by the light directly absorbed by the {PDI-Py} moiety and not upon excitation of the Ru(II) complex. Taken together

with the information provided by the excitation spectrum, the latter result shows that an energy transfer process from  $\{[\text{Ru}(\text{phen})_3]^{2+}\}$  to the  $^1\text{PDI-Py}$  state is not operative.

#### 4. Solvatochromism

To confirm the solvatochromic behavior, the absorption and emission of PDI-Py and RuPDI-Py were further measured in various solvents of different polarities at room temperature and in a glass matrix at 77 K (Figure S14). The absorption spectra were almost identical in the examined solvents, showing only a small hypsochromic shift of the  $S_0 \rightarrow S_1$  band in THF for both compounds analyzed. On the other hand, the emission peak wavelength showed strong solvent dependence, being blue-shifted upon decreasing polarity. For example, the PDI-Py emission maximum was blue-shifted, with respect to DMSO, to 755 nm ( $\sim 25$  nm) ( $\Phi_{\text{fl}} = 0.01$  and  $\tau_{\text{fl}} = 2.80$  ns) in a nonpolar solvent such as dichloromethane (DCM) and to 747 nm ( $\sim 37$  nm) ( $\tau_{\text{fl}} = 4.80$  ns) in a glass matrix at 77 K, indicating the CT character of the lowest singlet excited state of PDI-Py. The solvatochromic behavior of the  $\{\text{PDI-Py}\}$  component was preserved in the RuPDI-Py dyad and it was similar to that observed for the PDPI-Py reference, i.e., the absorption spectrum of RuPDI-Py was not significantly influenced by the solvent whereas the fluorescence spectrum was blue-shifted to 765 nm ( $\sim 22$  nm) ( $\tau_{\text{fl}} = 2.40$  ns) in dichloromethane and to 750 nm ( $\sim 37$  nm) ( $\tau_{\text{fl}} = 4.84$  ns) in a glass matrix at 77 K.

## Scheme, Figures and Tables



Scheme S1. Synthetic route to PDI-Py ligand.

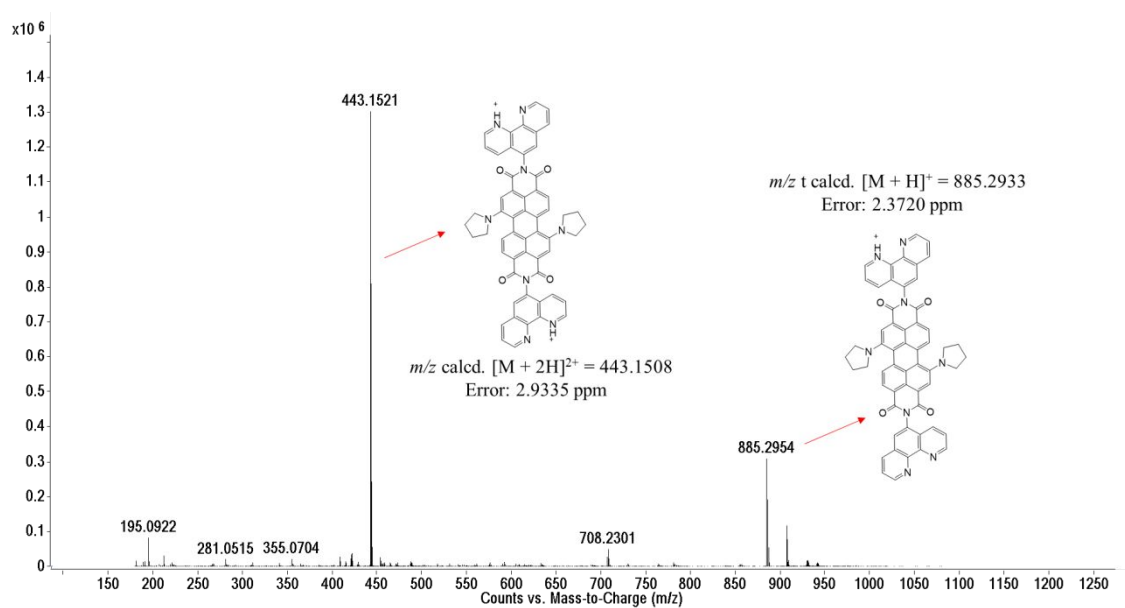
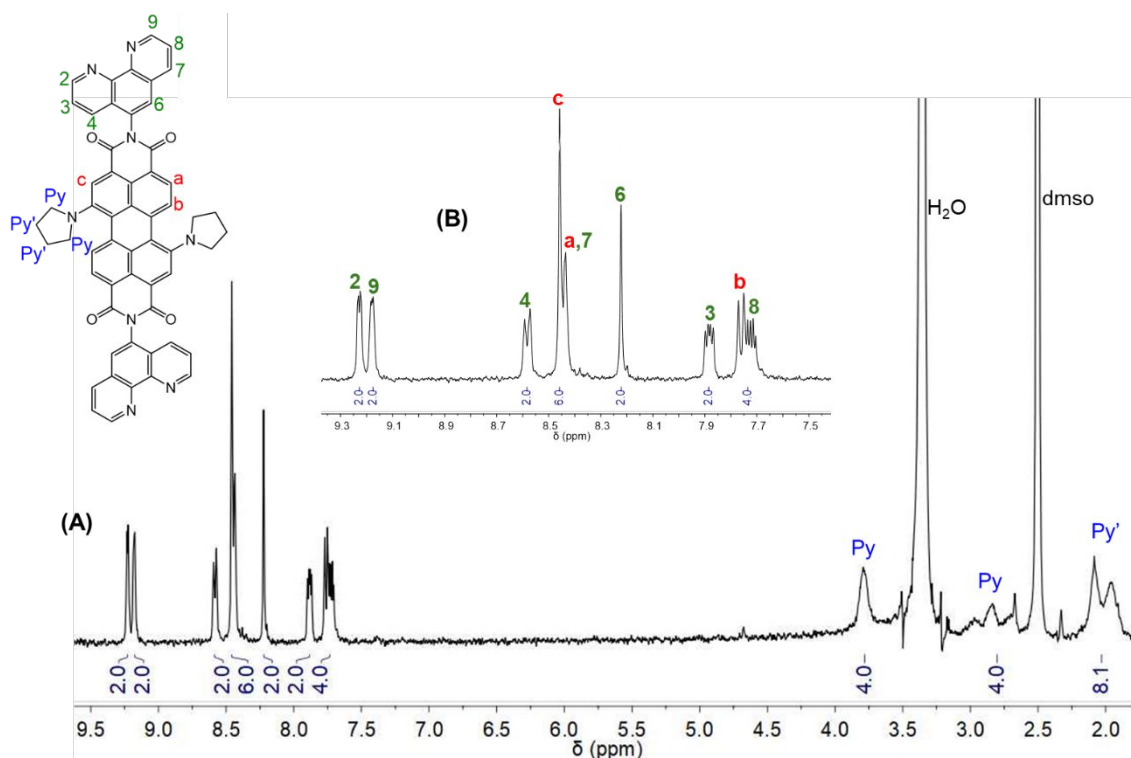


Figure S1. ESI(+)-MS spectrum of PDI-Py ligand in methanol.

Table S1.  $^1\text{H}$  and  $^{13}\text{C}$  NMR chemical shifts ( $\delta$ ) of the PDI-Py ligand in  $\text{DMSO-d}_6$  at 600 MHz.

Proton	$^1\text{H}$ /ppm	COSY/ppm	$^{13}\text{C}$ /ppm (via HSQC)	$^1\text{H} - ^{13}\text{C}$ HMBC
2	9.23	7.88	150.1	136.7
3	7.88	8.58; 9.23	123.6	127.1
4	8.58	7.78	136.1	127.1; 145.9; 150.1
6	8.22	-	127.1	132.0; 136.1; 145.9
7, a	8.43	7.75; 7.72	126.2; 131.4	122.0; 145.9; 149.9
8	7.72	8.42; 9.17	123.2	116.9; 131.4; 129.8
9	9.18	7.72	149.9	123.5
b	7.76	8.44	123.5	116.9; 118.5; 129.8
c	8.46	-	120.0	122.0; 163.9
Py	3.78	-	50.7	-
Py	2.85	-	50.7	-
Py'	1.80-2.20	-	25.6	-



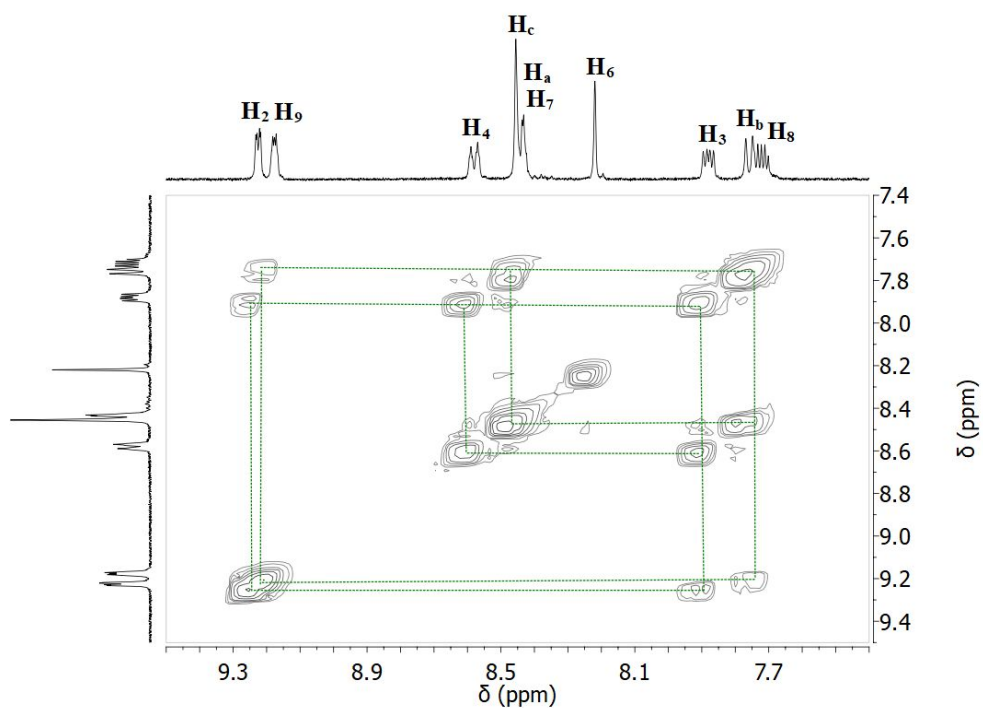


Figure S3. Aromatic region in the  $^1\text{H}$ - $^1\text{H}$  COSY NMR spectrum of the PDI-Py ligand (600 MHz, DMSO- $d_6$ ).

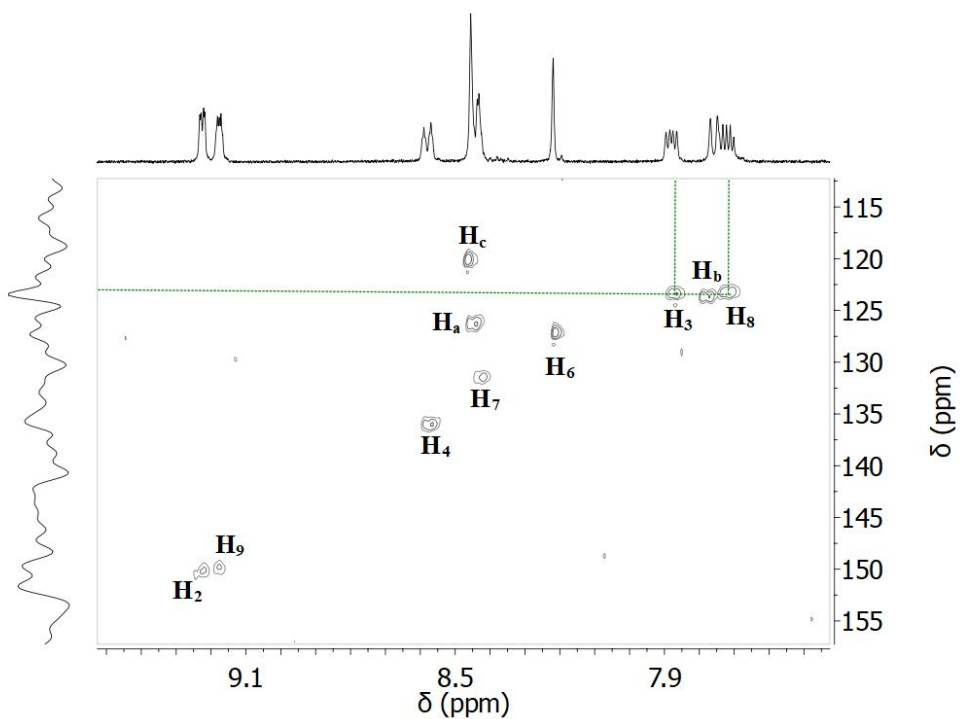


Figure S4. Aromatic region in the  $^1\text{H}$ - $^{13}\text{C}$  HSQC NMR spectrum of the PDI-Py ligand (600 MHz, DMSO- $d_6$ ).

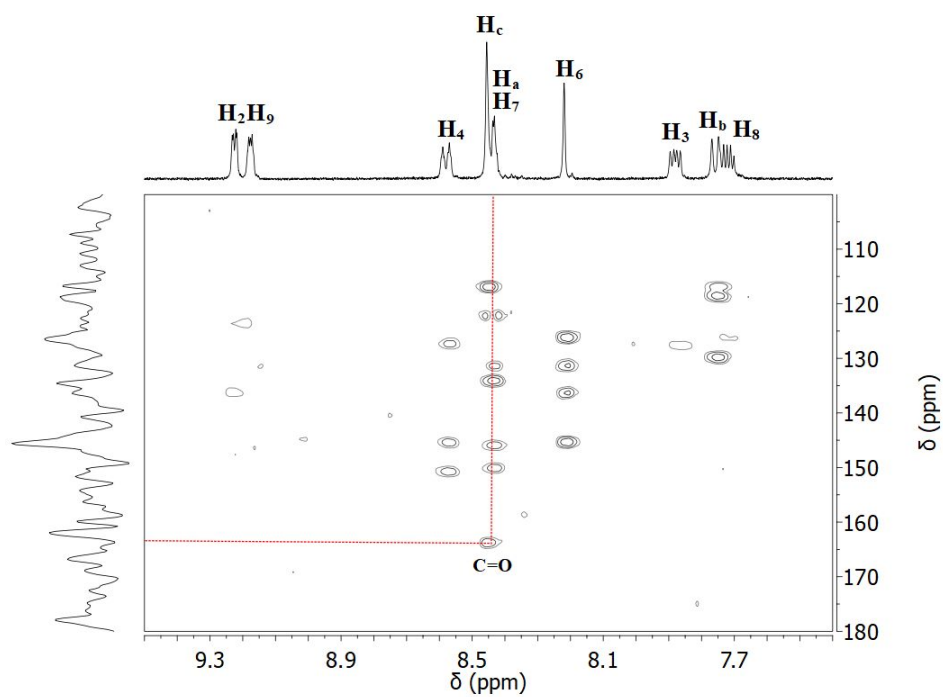
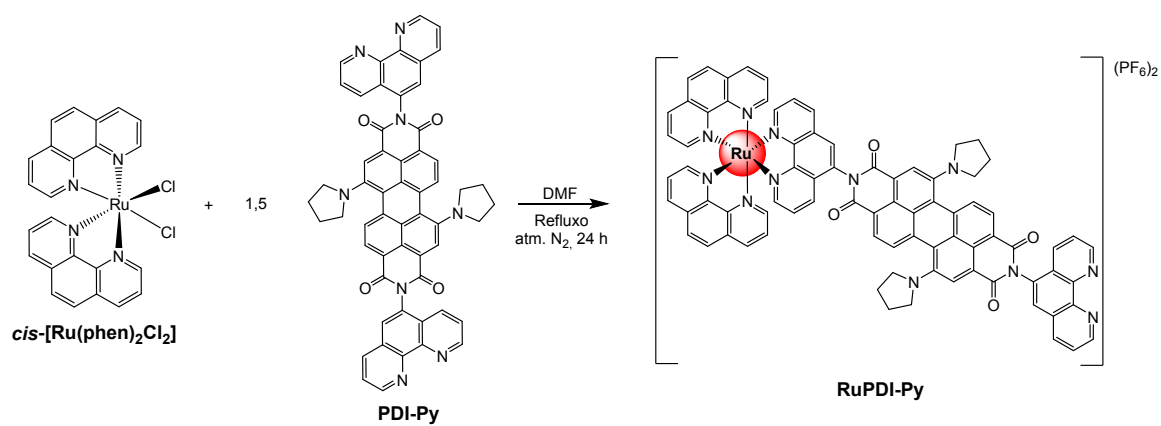


Figure S5. Aromatic region in the  $^1\text{H}$ - $^{13}\text{C}$  HMBC NMR spectrum of the PDI-Py ligand (600 MHz, DMSO- $d_6$ ).



Scheme S2. Synthetic route to RuPDI-Py dyad.

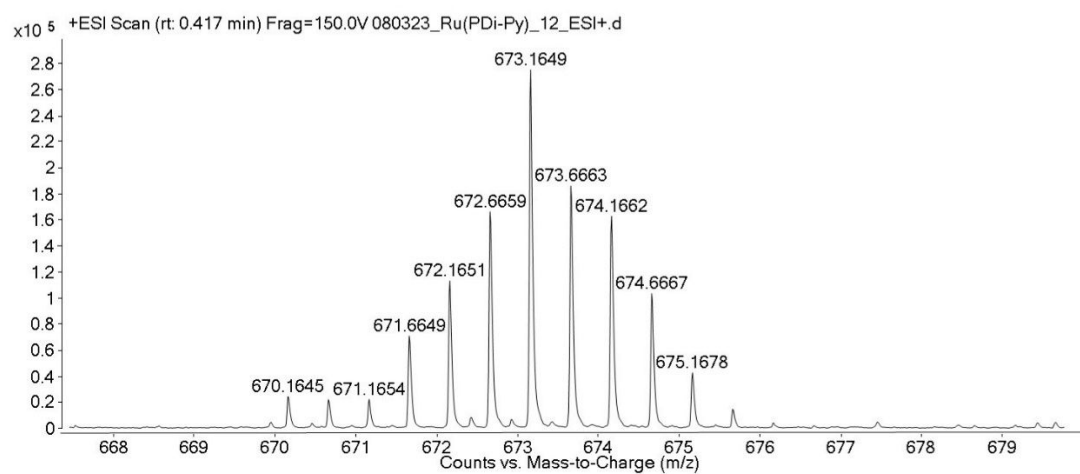
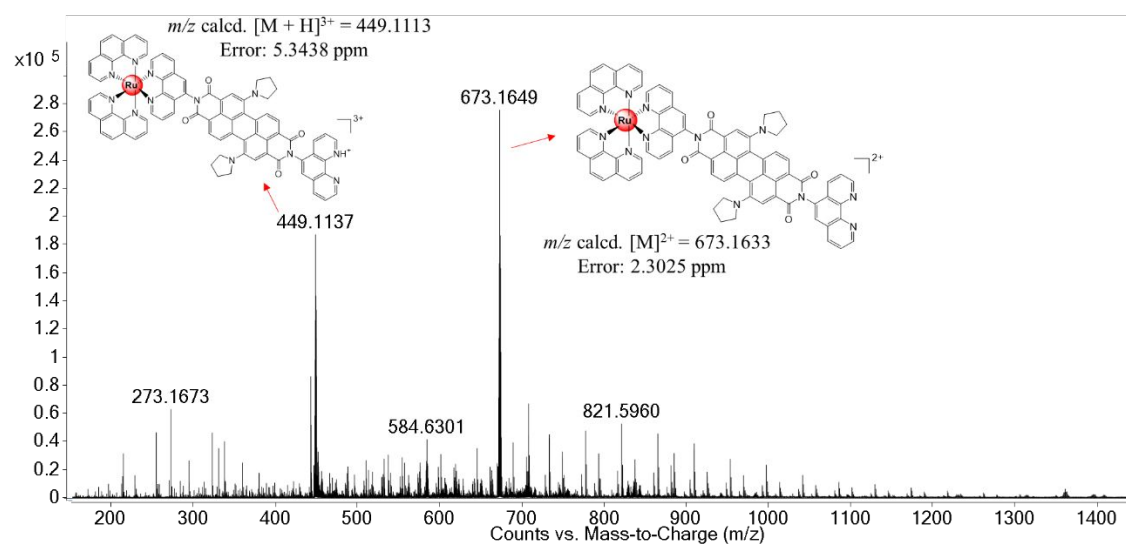


Figure S6. ESI(+)-MS spectrum of RuPDI-Py dyad in acetonitrile (top) and spectrum expansion on  $[M]^{2+}$  ion,  $m/z = 673.1649$  highlighting Ruthenium isotopic distribution (bottom).

Table S2. <sup>1</sup>H and <sup>13</sup>C NMR chemical shifts of the RuPDI-Py dyad in DMSO-d<sub>6</sub> at 600 MHz.

Proton	<sup>1</sup> H /ppm	COSY/ppm	<sup>13</sup> C/ppm (via HSQC)	<sup>1</sup> H - <sup>13</sup> C HMBC
<b>phen-PDI</b>				
2	9.23	7.8	150.6	124.4; 137.2; 146.1
3	7.88	8.57; 9.23	124.3	128.6
4	8.58	7.78	136.1	127.12; 145.9; 150.1
6	8.21		128.4	132.2; 146.1
7	8.42		132.3	
8	7.72		124.3	117.3; 119.1; 130.9
9	9.18	7.72	151.4	124.4; 146.1
<b>phen-PDI/Ru</b>				
2'	8.85	7.80	136.4	128.8; 147.8; 153.2
3', 8'	7.64 – 7.73		124.3	
4', 7'	8.14 – 8.23	7.80	153.5	127.1; 137.2; 147.7
6'	8.66		126.5	128.5; 134.0; 137.3; 147.7
9'	8.78		133.5	128.8; 147.8; 153.2
<b>phen-Ru</b>				
2'', 9''	8.82	7.86	137.5	147.8; 153.2
3'', 8''	7.86		126.9	130.9; 153.3
4'', 7''	8.12	7.86	153.5	127.0; 137.2; 147.7
5'', 6''	8.42		128.4	122.7; 130.9; 147.7; 151.1
<b>PDI-Py</b>				
a, a'	8.43 – 8.50	7.65– 7.77	126.8	
b, b'	7.65 – 7.77	8.43– 8.50	124.3	
c, c'	8.43 – 8.50		120.8	164.4
Py	3.79		52.8	
Py	2.85		52.8	
Py'	1.80-2.20		25.5	

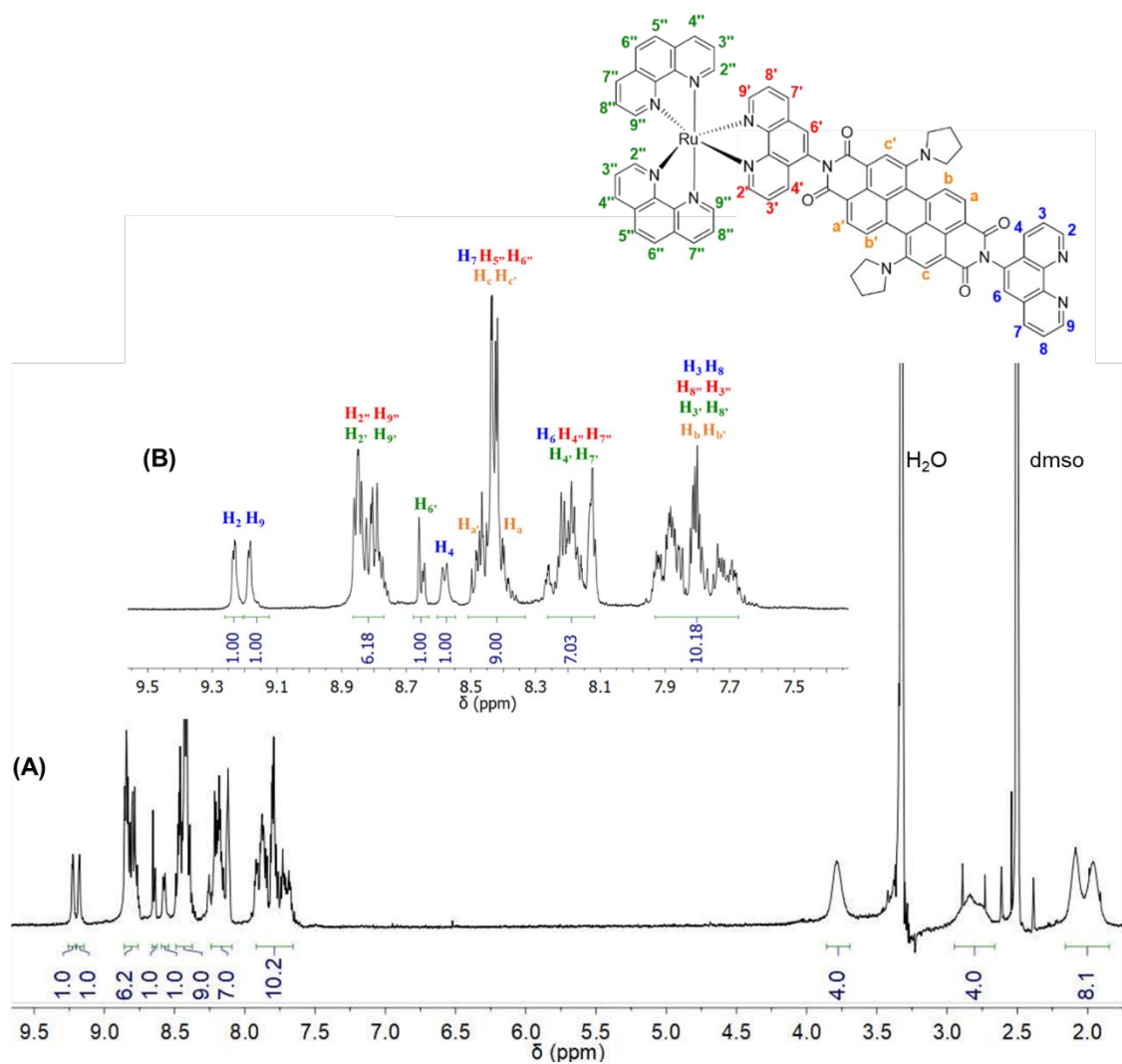


Figure S7. (A)  $^1\text{H}$  NMR spectrum of RuPDI-Py dyad in DMSO- $d_6$  at 298K, with insertion (B) of the deshielding region of the spectrum. Insertion of the chemical structure of RuPDI-Py dyad.

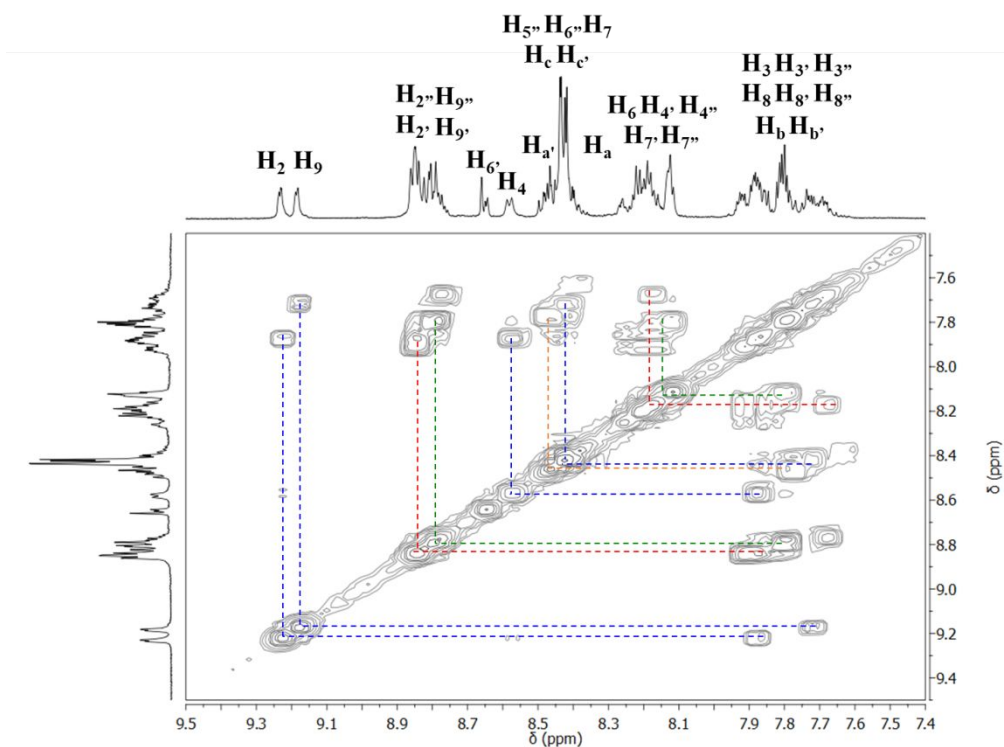


Figure S8. Aromatic region in the  $^1\text{H}$ - $^1\text{H}$  COSY NMR spectrum of the RuPDI-Py dyad (600 MHz, DMSO- $d_6$ ).

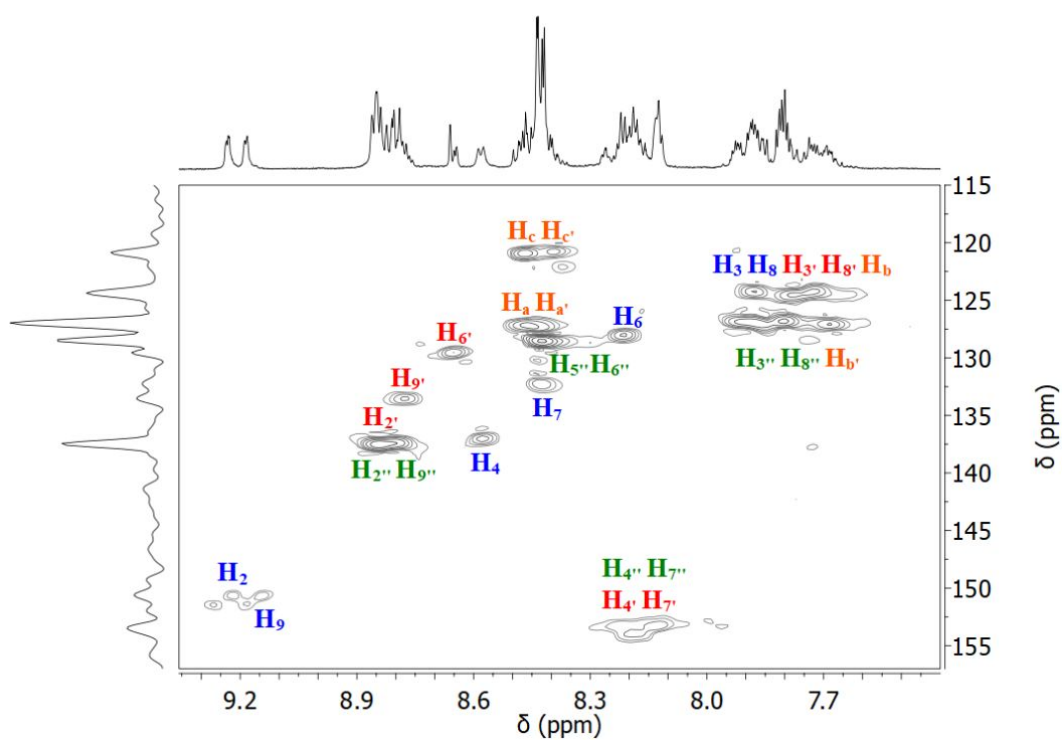


Figure S9. Aromatic region in the  $^1\text{H}$ - $^{13}\text{C}$  HSQC NMR spectrum of the RuPDI-Py dyad (600 MHz, DMSO- $d_6$ ).

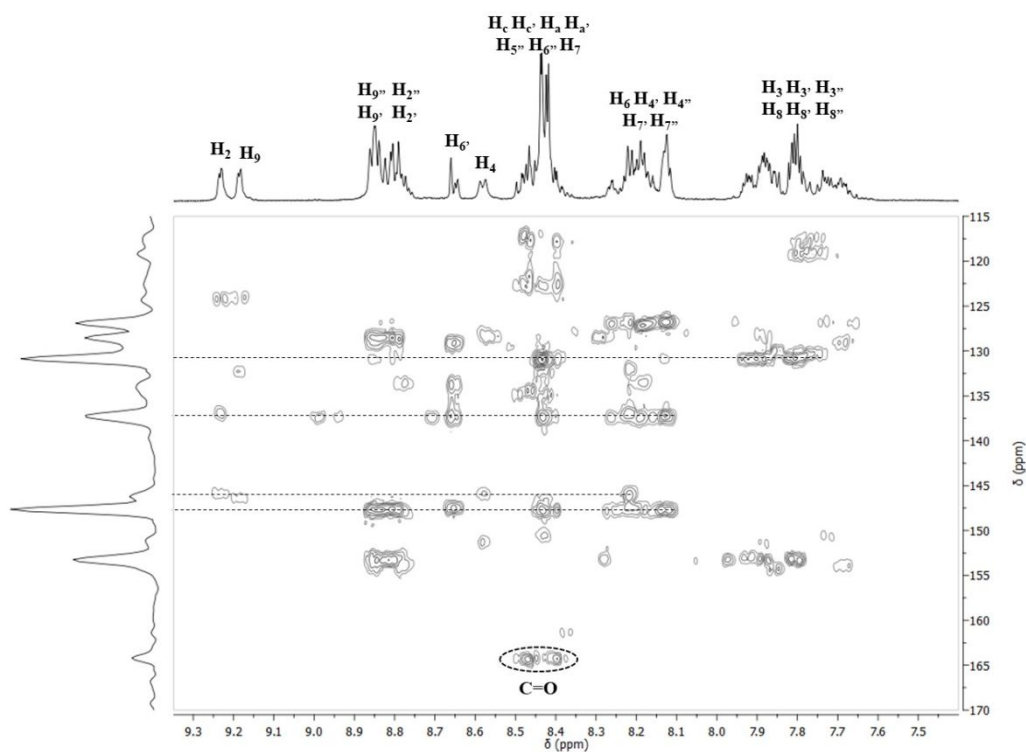


Figure S10. Aromatic region in the  $^1\text{H}$ - $^{13}\text{C}$  HMBC NMR spectrum of the RuPDI-Py dyad (600 MHz, DMSO- $d_6$ ).

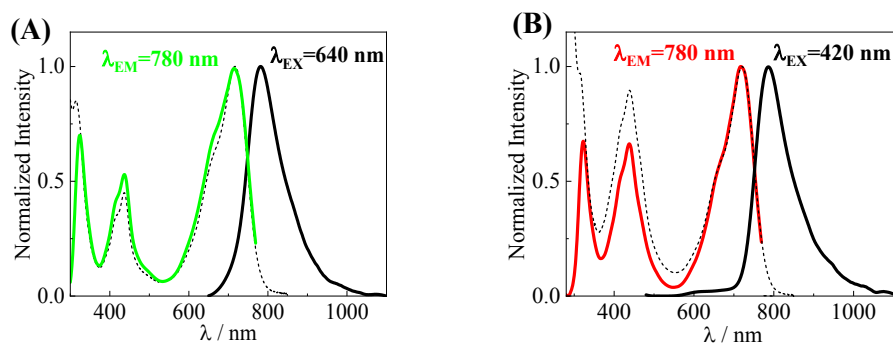


Figure S11 – Comparison of the absorption (dashed black-line), emission (solid black line), and excitation (colored line) spectra of the PDI-Py (A) and RuPDI-Py (B) in deaerated DMSO solution ( $c = 20 \mu\text{M}$ ), except from excitation spectra that were registered for solutions with  $A < 0.1$  in the investigated spectral range.

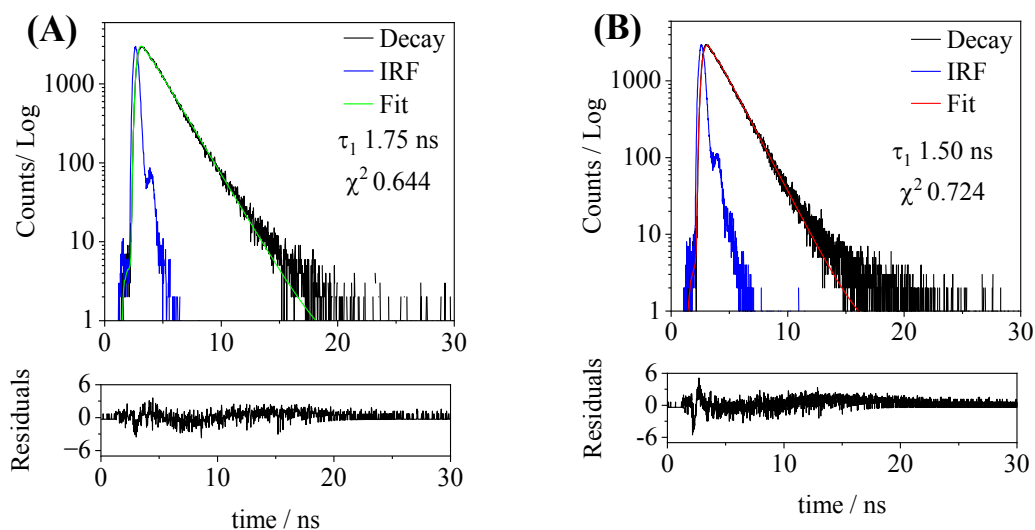


Figure S12. Time-resolved emission profiles for PDI-Py (A) and RuPDI-Py (B) with  $\lambda_{\text{EX}} = 640$  nm and  $\lambda_{\text{EM}} = 780$  nm in deaerated DMSO solution ( $c = 20 \mu\text{M}$ ).

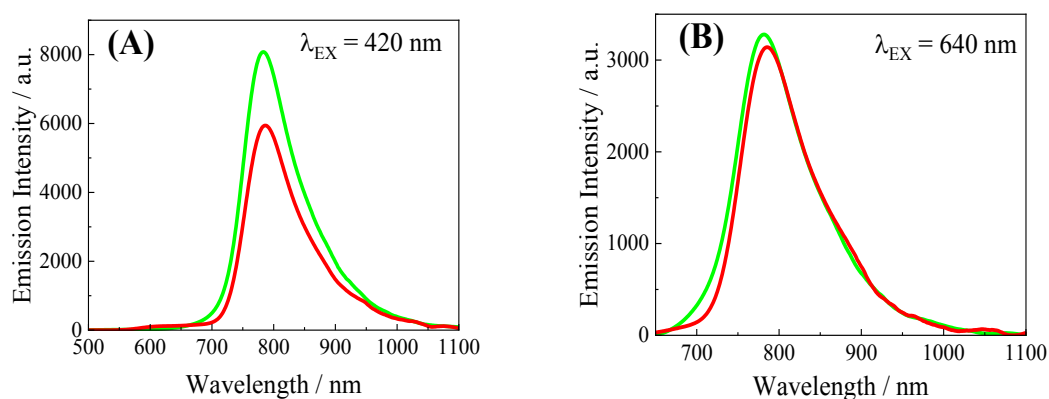


Figure S13. Comparison of emission spectra of RuPDI-Py (red) and PDI-Py (green) obtained from optically matched solutions ( $\text{abs} = 0.1$  at the excitation wavelength) in deaerated DMSO solution. A:  $\lambda_{\text{exc}} = 420$  nm; B:  $\lambda_{\text{exc}} = 640$  nm

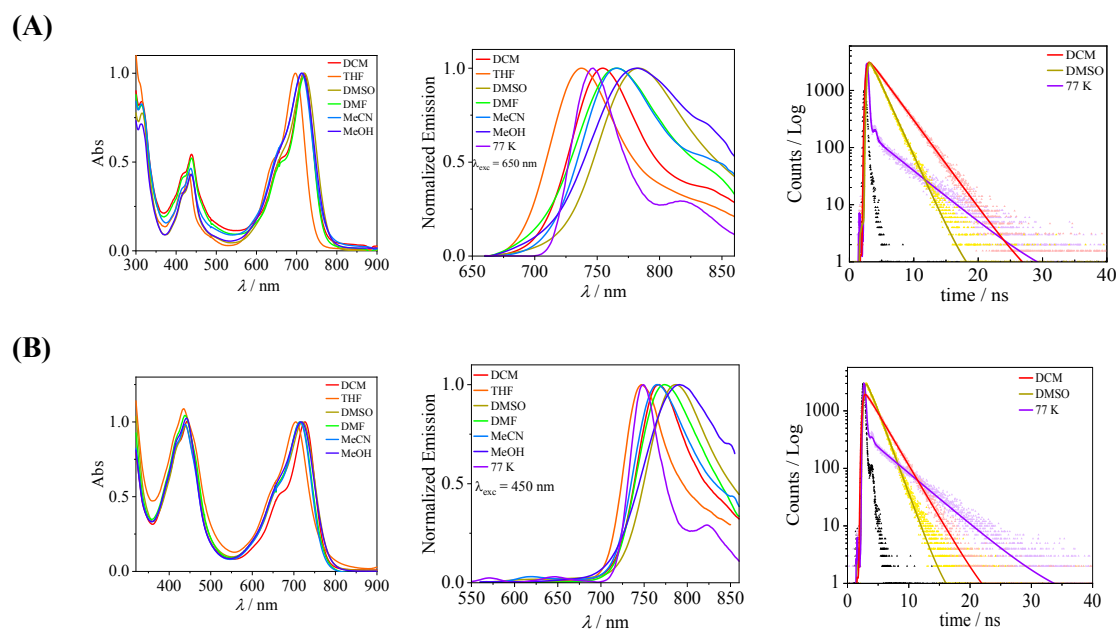


Figure S14. Absorption, emission spectra and emission lifetime decay profiles of PDI-Py (A) and RuPDI-Py (B) in different organic solvents at room temperature (aerated solutions), and in butyronitrile glass at 77 K. The emission lifetimes were measured at  $\lambda_{\text{exc}} = 640 \text{ nm}$  and  $\lambda_{\text{em}} = 780 \text{ nm}$  in aerated solutions.

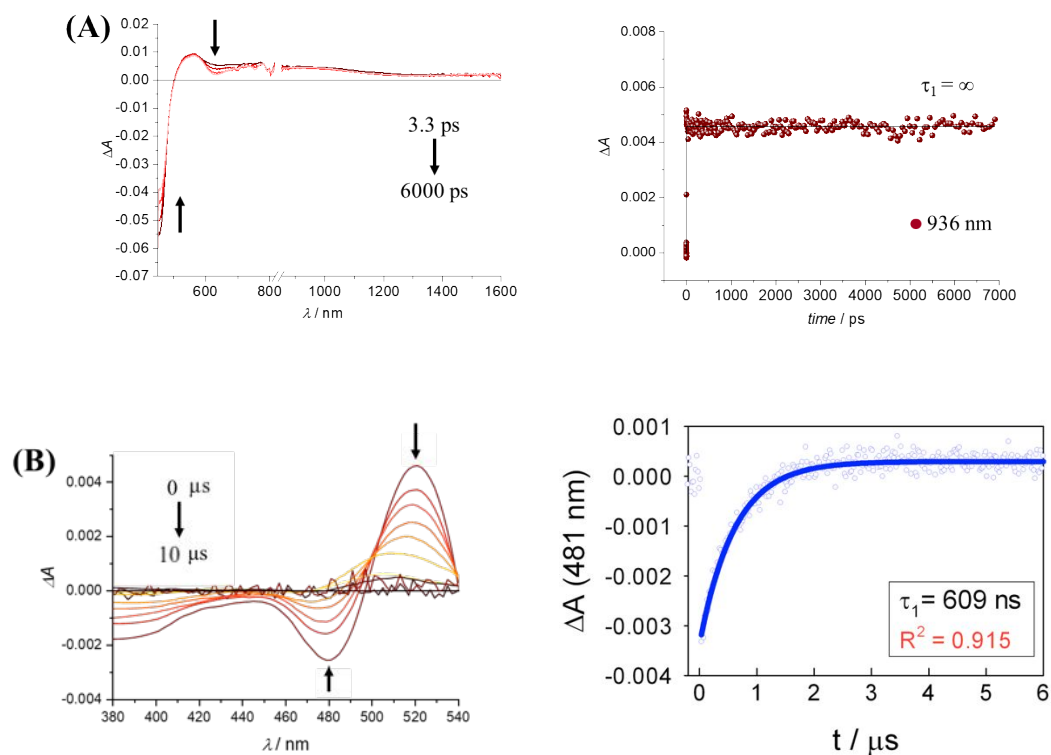


Figure S15. Femtosecond transient absorption spectroscopy with  $\lambda_{\text{exc}} = 450 \text{ nm}$  (A) and nanosecond transient absorption spectroscopy with  $\lambda_{\text{exc}} = 355 \text{ nm}$  (B) of the  $[\text{Ru}(\text{phen})_3]^{2+}$  reference in DMSO: spectral evolution and kinetic analysis at selected wavelengths.

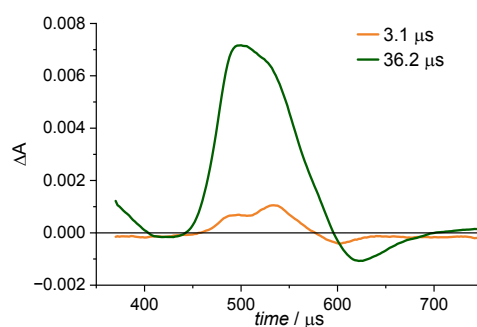


Figure S16. Spectral distribution of the amplitudes of the calculated lifetimes from global fit analysis of the nanosecond transient absorption matrix of the RuPDI-Py dyad excited at 355 nm in DMSO under oxygen-free conditions.

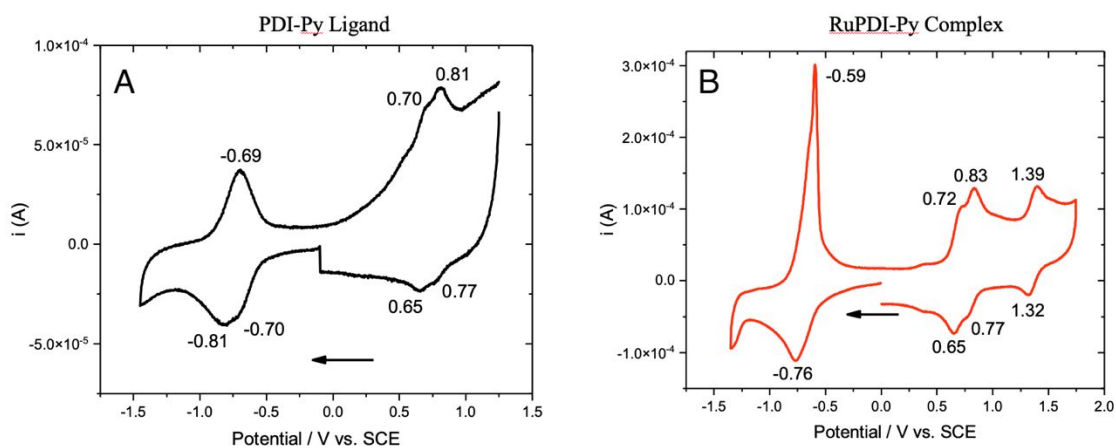


Figure S17. Cyclic voltammogram of PDI-Py (A) and RuPDI-Py (B) in  $\text{CH}_3\text{CN}$  solutions at 2 V/s. TBAPF<sub>6</sub> was used as a supporting electrolyte; ferrocene was added to the same solutions as in internal reference (0.40 V vs. SCE).

Table S3. Halfwave potentials vs. SCE for the analysed compounds in  $\text{CH}_3\text{CN}$ .

Compound	$E_{\text{red},1} / \text{V}$	$E_{\text{ox},1} / \text{V}$	$E_{\text{ox},2} / \text{V}$	$E_{\text{ox},3} / \text{V}$
$[\text{Ru}(\text{phen})_3]^{2+}$ <sup>a</sup>	-1.41 <sup>p</sup>	1.40 <sup>p</sup>	-	-
PDI-Py	-0.70 <sup>p</sup>	0.70 <sup>p</sup>	0.81 <sup>p</sup>	-
RuPDI-Py	-0.76 <sup>p</sup>	0.68	0.80	1.35

<sup>a</sup> See Reference XX (Tokel-Takvoryan, N. E.; Hemingway, R. E.; Bard, A. J. Electrogenerated Chemiluminescence. XIII. Electrochemical and Electrogenerated Chemiluminescence Studies of Ruthenium Chelates. *J. Am. Chem. Soc.* **1973**, 95 (20), 6582–6589)

<sup>p</sup> Peak potentials.

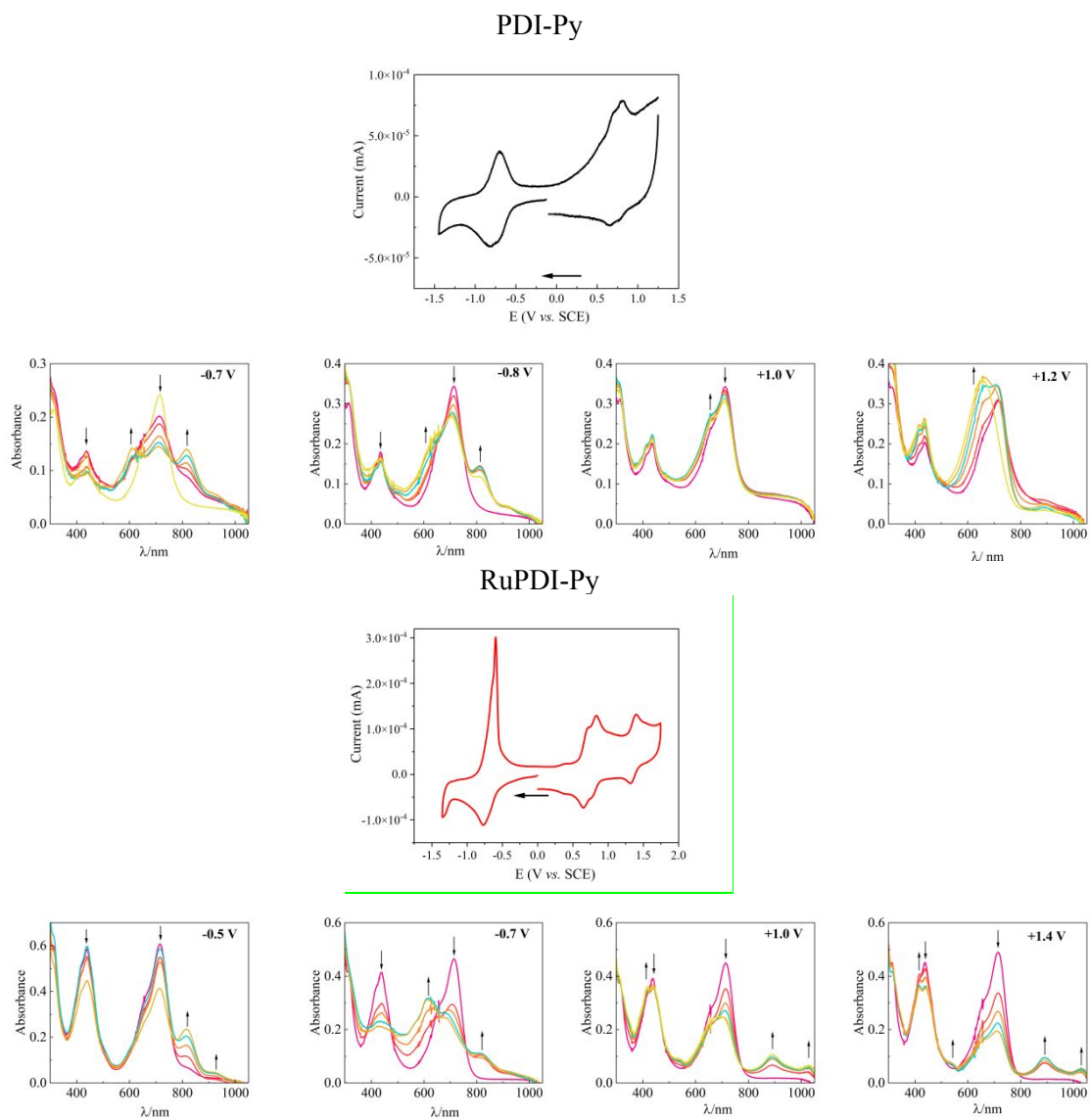


Figure S18. Spectroelectrochemical analyses for PDI-Py and RuPDI-Py in degassed CH<sub>3</sub>CN at several applied potentials.

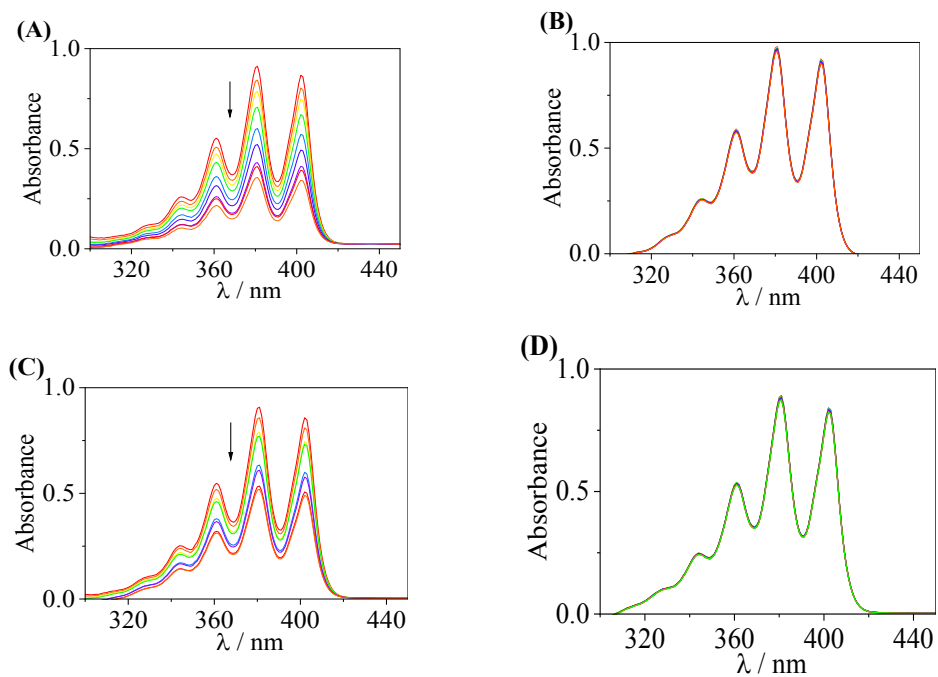


Figure S19. Bleaching of DMA (100  $\mu\text{M}$ ) in DMSO upon irradiation at 450 nm in the presence of the RuPDI-Py dyad (A), PDI-Py ligand (B),  $[\text{Ru}(\text{phen})_3]^{2+}$  reference (C), and DMA control (D) (irradiation time = 30 minutes).

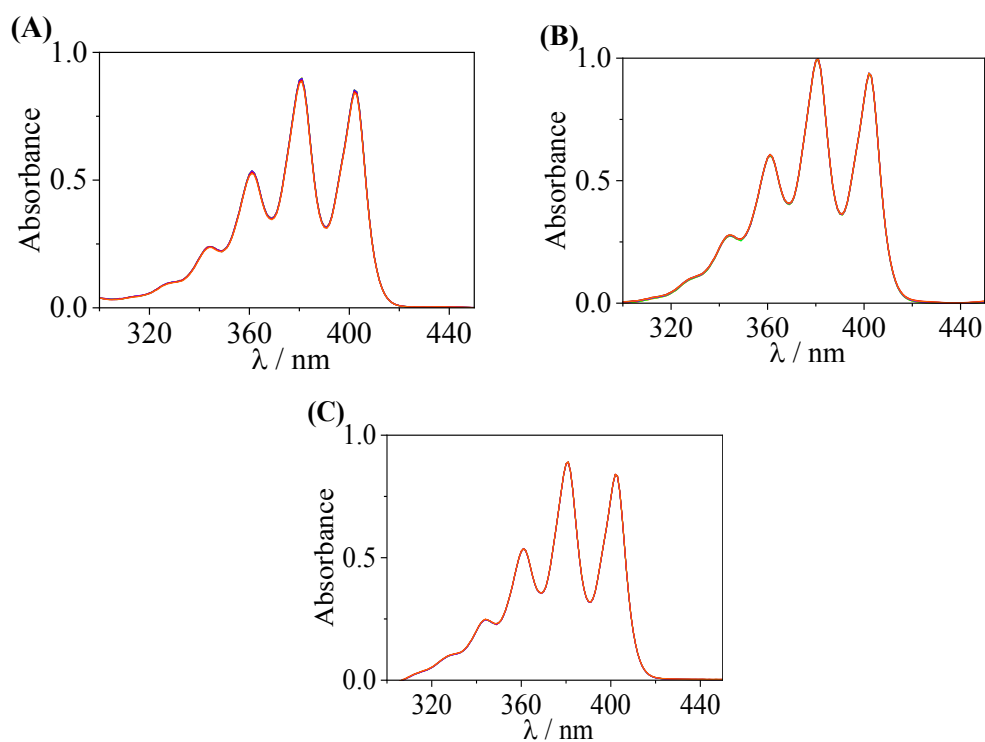


Figure S20. Bleaching of DMA in DMSO upon irradiation at 720 nm in the presence of the RuPDI-Py dyad (A), PDI-Py ligand (B), and DMA control (C) (irradiation time = 30 minutes).

## References

- (1) Würthner, F. Preparation and Characterization of Regioisomerically Pure 1,7-Disubstituted Perylene Bisimide Dyes. *Journal of Organic Chemistry* **2004**, *69* (23), 7933–7939. <https://doi.org/10.1021/JO048880D>.
- (2) Işık Büyükekşi, S.; Şengül, A.; Erdönmez, S.; Altındal, A.; Orman, E. B.; Özkaya, A. R. Spectroscopic, Electrochemical and Photovoltaic Properties of Pt(II) and Pd(II) Complexes of a Chelating 1,10-Phenanthroline Appended Perylene Diimide. *Dalton Transactions* **2018**, *47* (8), 2549–2560. <https://doi.org/10.1039/C7DT04713D>.